Modelling of Bundle Divertors - II

G.A. Emmert and A.W. Bailey

July 1980

UWFDM-365

FUSION TECHNOLOGY INSTITUTE

UNIVERSITY OF WISCONSIN

MADISON WISCONSIN

Modelling of Bundle Divertors - II

G.A. Emmert and A.W. Bailey

Fusion Technology Institute
University of Wisconsin
1500 Engineering Drive
Madison, WI 53706

http://fti.neep.wisc.edu

July 1980

UWFDM-365

MODELLING OF BUNDLE DIVERTORS - II

G. A. Emmert and A. W. Bailey

Fusion Engineering Program
Nuclear Engineering Department
University of Wisconsin
Madison, Wis. 53706

July 1980

UWFDM-365

Abstract

The bundle divertor differs from the poloidal divertor in that it has a strong magnetic mirror in the entrance to the divertor chamber. This affects the flow of plasma from the scrape-off zone into the divertor chamber and the backflow of ions from the divertor chamber into the main chamber. The magnetic hill and subsequent well causes an electrostatic potential along the field lines; this traps cold ions in the divertor chamber. Ionization of neutral gas in the divertor chamber reduces the electrostatic well; maintaining a well then implies an upper limit on the neutral gas density. In this work, the effect of ionization on the potential profile is calculated and an estimate of the allowable neutral pressure is given.

A feature of the bundle divertor [1], in comparison with the poloidal divertor, is the strong magnetic mirror at the divertor throat. A typical mirror ratio is of the order of 3 to 4 for both the DITE [1] and ISX [2] bundle divertors. Depending on the details of the design, the field in the divertor chamber can drop below that in the main chamber, so that the mirror ratio seen from the divertor chamber is even larger. This magnetic topology has an effect on the performance of the bundle divertor. The magnetic mirror reflects some of the escaping ions back into the main chamber (those outside the loss cone) and increases the electrostatic potential in the scrape-off zone relative to the target plate. This has the effect of increasing the energy lost per electron reaching the target plate and thereby acts to reduce the electron temperature in the scrape-off zone. The magnetic mirror also produces an electrostatic potential drop along the field line between the scrape-off zone and the divertor chamber (separate from the sheath potential drop). Cold ions (fuel + impurities) in the divertor chamber are then electrostatically trapped and cannot flow back from the divertor chamber to the main chamber. These effects are discussed in Ref. 3.

In this paper we consider in more detail the effect of a neutral gas in the divertor chamber on the electrostatic potential. Ionization of the gas by the hot plasma flowing from the scrape-off zone into the divertor chamber produces a cold plasma which reduces the potential drop between the divertor chamber and the main chamber. The amount of cold plasma produced is dependent on the neutral pressure; consequently one obtains a limit on the allowed neutral pressure in order to maintain the electrostatic trap. This has implications for the vacuum pumping system in the divertor chamber. A high

neutral gas density in the divertor chamber also has the desirable effect of defocussing the energy flux in the escaping hot plasma by charge exchange with the neutral gas. This spreads the power density incident on the target plate over a large area.

In order to make the problem analytically tractable, the magnetic field profile along a field line as it passes from the scrape-off zone into the divertor chamber is modelled as shown in Fig. 1. Neglecting cold plasma effects, the electrostatic potential drops across the mirror throat, as shown in Fig. 1. This result is taken from Ref. 3. We let S(x) be the number of cold ions produced per unit volume per unit time in the divertor chamber by ionization. The density of cold ions, $n_c(x)$, due to the source is given by [3]:

$$n_c(x) = \left(\frac{M}{2e}\right)^{1/2} \int_0^x \frac{dx' \; S(x')}{[\phi(x') - \phi(x)]^{1/2}} \quad , \tag{1}$$

where e is the charge and M is the mass. Quasineutrality in the divertor chamber requires

$$n_e(x) = n_H(x) + n_c(x) \quad . \tag{2}$$

For the electron density, we take a Boltzmann distribution along the field line:

$$n_e(x) = n_u \exp(e\phi(x)/T_e) \quad . \tag{3}$$

The upstream density is n_u and the upstream potential has been defined to be

zero. The hot ion density in the divertor chamber is reduced from n_u by the expansion of the magnetic field and by acceleration of the ions by the electric field. This has been evaluated in Ref. 3. We use a simpler formula which is a good approximation to the result calculated in Ref. 3, but allows us to evaluate some integrals analytically:

$$n_H(x) = \frac{n_u\sqrt{T_H}}{R_d[-\pi e\phi(x) + T_H(1 + \pi - \pi/R_d)]^{1/2}} \quad . \tag{4}$$

T_H is the hot ion temperature and $R_d = B_d/B_t$. This is essentially the same as that used by Baldwin and Logan [4] for thermal barriers in tandem mirrors, except that it contains an additional term due to the acceleration of the ions by the decreasing field. Putting Eqs. 1-4 together gives the result:

$$g(\psi) \equiv e^{-\psi} e^{-\psi_t} - \frac{1}{R_d[\pi\tau(\psi + b)]^{1/2}} = \frac{\lambda}{\pi}\int_0^s \frac{h(s')\,ds'}{[\psi(s) - \psi(s')]^{1/2}} \quad , \tag{5}$$

where

$$\psi = -e(\phi - \phi_t)/T_e \quad ,$$

$$\psi_t = e\phi_t/T_e \quad ,$$

$$\lambda = \pi S_0 L(M/2T_e)^{1/2}/n_u \quad ,$$

$$b = \psi_t + (1 - 1/R_d)/\tau + 1/(\pi\tau) \quad ,$$

and

$$s = x/L \quad .$$

The source function S(x) has been written as:

$$S(x) = S_0 h(x) \quad ,$$

where S_0 is the average value and $h(x)$ carries the profile information. Its profile is determined by the neutral gas density profile. We require only that $n(0) \simeq 0$ so that ionization for $x < 0$ can be neglected. The parameter ϕ_t is the jump in ϕ where the field drops and is determined by requiring that Eq. 5 be satisfied at $s = 0$; ϕ_t is thus related to S_0.

Since the left hand side of Eq. 5 does not contain s explicitly, it is convenient to interchange the dependent and independent variables and solve for $s = s(\psi)$. Equation 5 can then be solved analytically; the problem is reduced to quadratures. Before proceeding, the role of charge exchange reactions in determining the potential needs to be discussed. Charge exchange removes hot ions and replaces them with cold ions. Unfortunately, including charge exchange introduces an explicit x-dependence in n_H which makes Eq. 5 impossible to solve analytically. Instead it must be solved numerically in conjunction with a neutral transport equation determining the neutral density profile. This is beyond the scope of the present work. Since the density of the hot ions removed by charge exchange is much less than that of the cold ions created, one can bound the effect of charge exchange by considering it as an ionization process; i.e. replace $\langle\sigma v\rangle_{ioniz}$ by $\langle\sigma v\rangle_{ioniz} + \langle\sigma v\rangle_{cx}$. This gives an upper limit on the reduction of the electrostatic well. We take this approach.

The solution of Eq. 5 is [5]:

$$\lambda h(s) \frac{ds}{d\psi} = \frac{d}{d\psi} \int_0^{\psi} \frac{g(\psi')}{(\psi - \psi')^{1/2}} d\psi' \quad .$$

Inserting $g(\psi)$ from Eq. 5 and evaluating the integrals gives:

$$\lambda h(s)\,\frac{ds}{d\psi} = e^{-\psi_t}\left[\frac{1}{\sqrt{\psi}} - 2e^{-\psi}\,D((\psi)^{1/2})\right] - \frac{1}{R_d(\psi + b)}\left(\frac{b}{\pi\tau\psi}\right)^{1/2} , \tag{6}$$

where $D(x) = \int_0^x \exp(t^2)\,dt$ is the Dawson function. The boundary condition at $s = 1$, the plasma edge of the sheath at the target plate, is $ds/d\psi = 0$ [6]; this determines $\psi_1 = \psi(1)$.

$$e^{-\psi_t}\left[\frac{1}{\sqrt{\psi_1}} - 2e^{-\psi_1}\,D((\psi_1)^{1/2})\right] = \frac{1}{R_d(\psi_1 + b)}\left(\frac{b}{\pi\tau\psi_1}\right)^{1/2} . \tag{7}$$

We next integrate Eq. 6 from $s = 0$ to $s = 1$, using $\int_0^1 h(s)\,ds = 1$, to get

$$\lambda = 2e^{-\psi_t}\,e^{-\psi_1}\,D((\psi_1)^{1/2}) - \frac{1}{R_d(\pi\tau)^{1/2}}\tan^{-1}\left[\left(\frac{\psi_1}{b}\right)^{1/2}\right] . \tag{8}$$

Equations 7, 8 and $\lambda = \pi S_0(M/2T_e)^{1/2}/n_u$, determine the jump ψ_t at $s = 0$, and the potential ψ_1 at the plasma side of the sheath as a function of the average cold ion source strength S_0.

The wall potential is then determined by equating the electron flux to the wall to the total ion flux incident on the wall. The hot ion flux is [3]

$$\Gamma_H = n_u\,\frac{F(R_u)}{R_d}\left(\frac{T_i}{2\pi M}\right)^{1/2} ,$$

where $R_u = B_t/B_u$, and $F(R_u)$ is computed in Ref. 3. The cold ion flux is simply $\Gamma_c = S_0 L$, and the electron flux is

$$\Gamma_e = n_u \left(\frac{T_e}{2\pi m}\right)^{1/2} \exp(-e\phi_w/T_e) \quad .$$

Thus, $\Gamma_H + \Gamma_c = \Gamma_e$, gives

$$\frac{e\phi_w}{T_e} = -\ln\left[\left(\frac{m}{M}\frac{T_i}{T_e}\right)^{1/2} \frac{F(R_u)}{R_d} + \left(\frac{2}{\pi}\frac{m}{M}\right)^{1/2} \lambda\right] \quad . \tag{9}$$

The potential profile in the divertor chamber is found by integrating Eq. 6 from zero to s and using the relationship between ψ_t and g found from Eqs. 7 and 8. The result is shown in Fig. 2 for various values of λ and a downstream mirror ratio of 4. Increasing values of λ (corresponding to increasing neutral gas density) cause the potential in the chamber to rise; the potential drop across the mirror throat decreases. At $\lambda = .5$, there is still a substantial electrostatic well in the divertor chamber. Fig. 3 shows more directly the effect of λ on the wall potential and on ψ_t. Figure 4 shows the effect of the downstream mirror ratio, R_d, on ψ_1, ψ_t, and ϕ_w at $\lambda = .5$. As the mirror ratio increases, the electrostatic well deepens somewhat and the upstream plasma potential relative to the wall increases. It should be noted that these results are independent of the neutral gas density profile in the divertor chamber, since no particular profile for h(s) was used, except in Fig. 2 where h(s) = 1 was used for illustrative purposes.

It is worthwhile to consider a specific application. One dimensional transport simulations [7] of an INTOR/ETF device suggest $n_u \simeq 3 \times 10^{12}$ cm^{-3}, $T_e \simeq T_i \simeq 2$ keV at the separatrix. For $R_d \simeq R_u \sim 4$, and $\lambda = .5$, the potential drop across the mirror throat is 1.3 kV, the potential drop between the mirror throat and the sheath edge is 1.2 kV, and the potential drop across the sheath

is 5.5 kV. The corresponding neutral density, n_0, can be determined from

$$S_0 L = \frac{\lambda n_u}{\pi} \left(\frac{2T_e}{M}\right)^{1/2}$$

and

$$S_0 \simeq n_u e^{-\psi_t} \langle\sigma v\rangle_e \, n_0 \quad .$$

Thus

$$n_0 L \simeq \frac{\lambda e^{\psi_t}}{\pi} \frac{1}{\langle\sigma v\rangle_e} \left(\frac{2T_e}{M}\right)^{1/2} \quad . \tag{10}$$

In this example, this gives $n_0 L \simeq 6.3 \times 10^{14}$ cm^{-2}. For a divertor chamber length $L \simeq 100$ cm, we have $n_0 \simeq 6.3 \times 10^{12}$ cm^{-3}. This is an (ill-defined) average density. It will be higher near the target plate and lower near the divertor throat. This corresponds to an average pressure of about 1.5×10^{-4} torr at room temperature.

If the scrape-off zone temperature were reduced to 50 eV by some unspecified mechanism, the neutral density at $\lambda = .5$ would be $n_0 L \simeq 6.3 \times 10^{13}$ cm^{-2}, a factor of 10 reduction. Clearly, the need for low temperature to reduce the plasma-wall interaction runs counter to the desire for high neutral pressure to reduce vacuum pumping speed requirements.

At too high a neutral pressure, the electrostatic potential can become higher in the divertor chamber than in the scrape-off zone. In this case the electric field drives the cold ions from the divertor chamber into the scrape-off zone. This regime cannot be obtained from the present analysis, however, because it assumes from the beginning that the potential is monotonically decreasing. This second regime (inverted potential profile) requires more analysis and will be the subject of a later paper.

Acknowledgement

The authors gratefully acknowledge stimulating conversations with Dr. Y.-K. M. Peng of Oak Ridge National Laboratory. This work was supported by the ETF Design Center at Oak Ridge National Laboratory.

References

1. P. E. Scott, C. M. Wilson, and A. Gibson, Nuclear Fusion 17, (1977) 481.
2. J. A. Rome, private communications.
3. G. A. Emmert, UWFDM-343, University of Wisconsin (1980).
4. D. E. Baldwin and B. G. Logan, Phys. Rev. Lett. 43, (1979) 1318.
5. J. W. Dettman, Mathematical Methods in Physics and Engineering, McGraw-Hill (1969), p. 410.
6. E. R. Harrison and W. B. Thompson, Proc. Phys. Soc. 74, (1959) 145.
7. W. A. Houlberg, private communication.

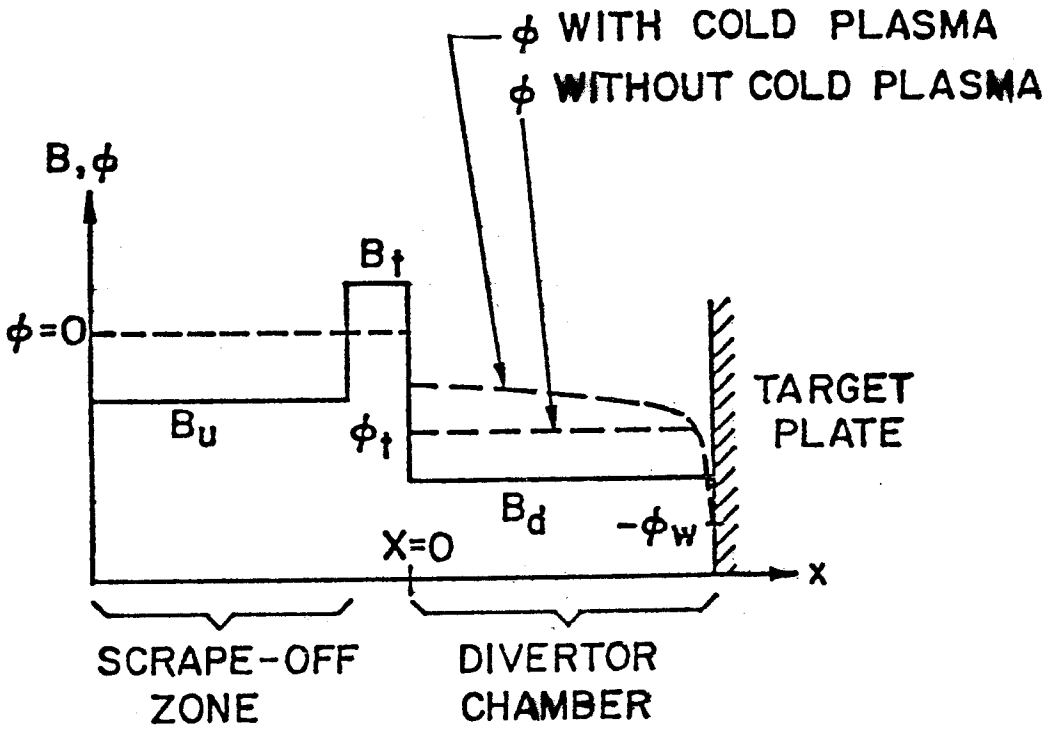

Fig. 1. One-dimensional model for the magnetic field strength and potential along a field line through the divertor.

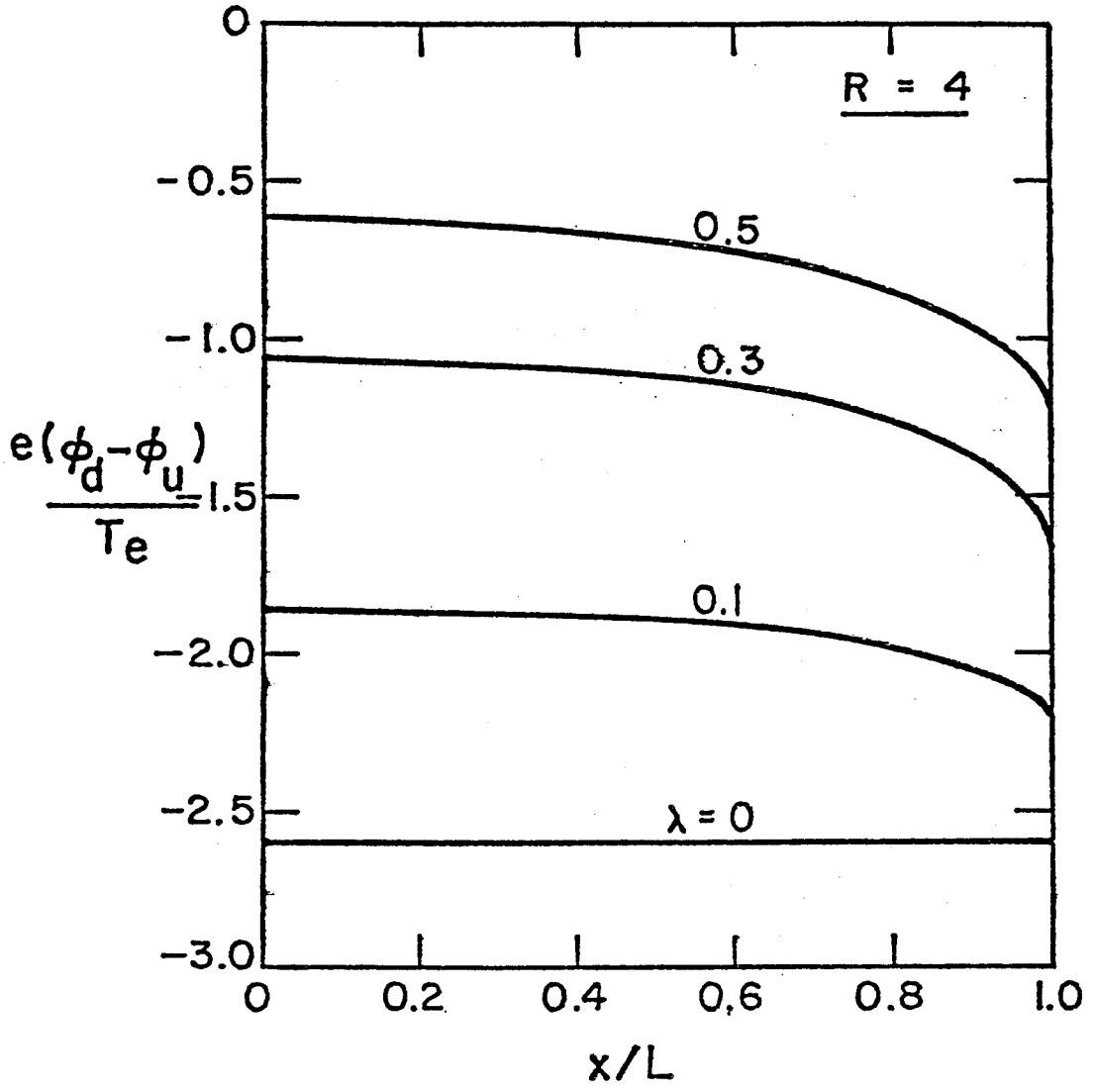

Fig. 2. The potential in the divertor chamber as a function of distance along the field line for various values of λ.

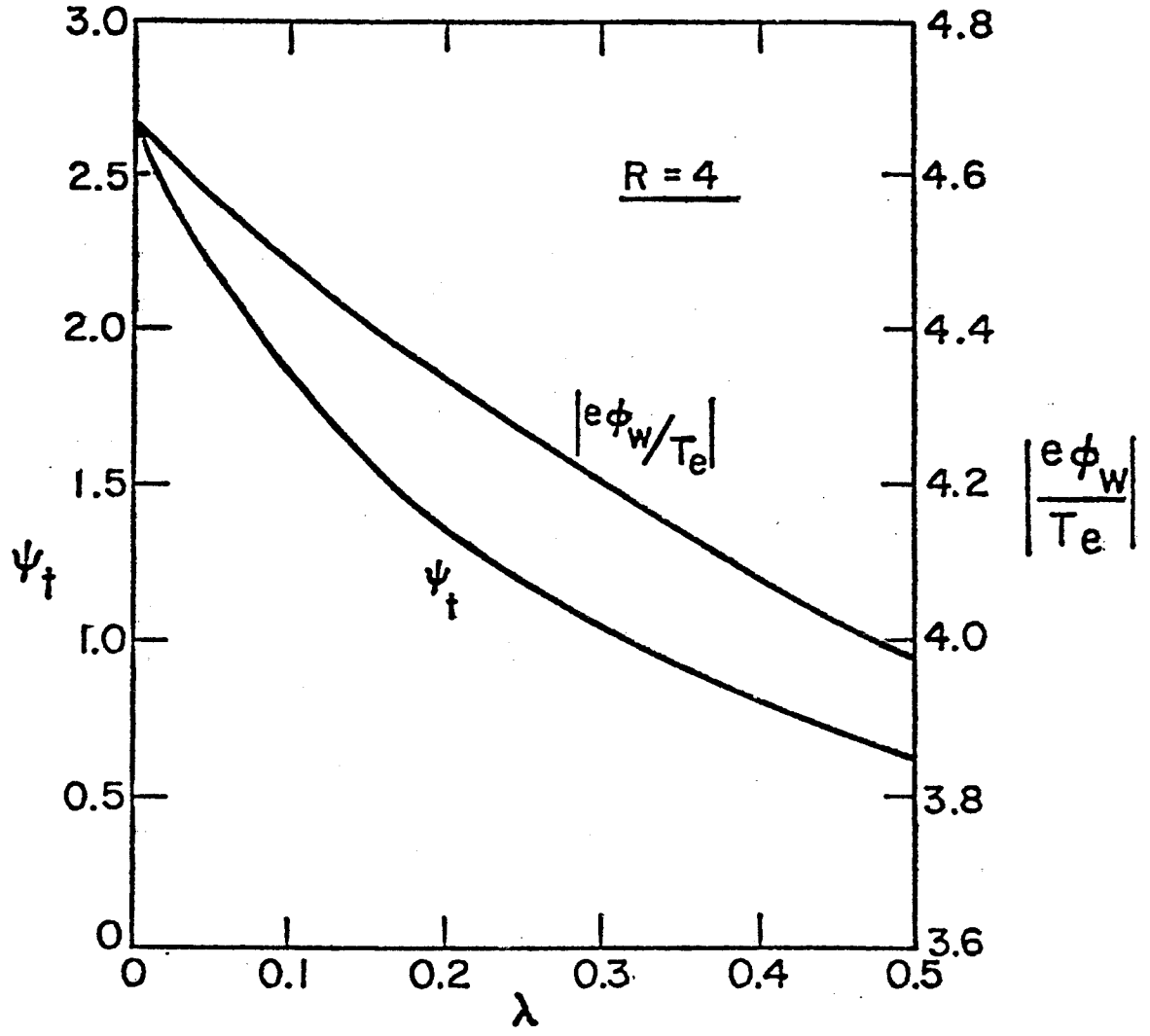

Fig. 3. The potential step at the divertor throat and the wall potential versus λ.

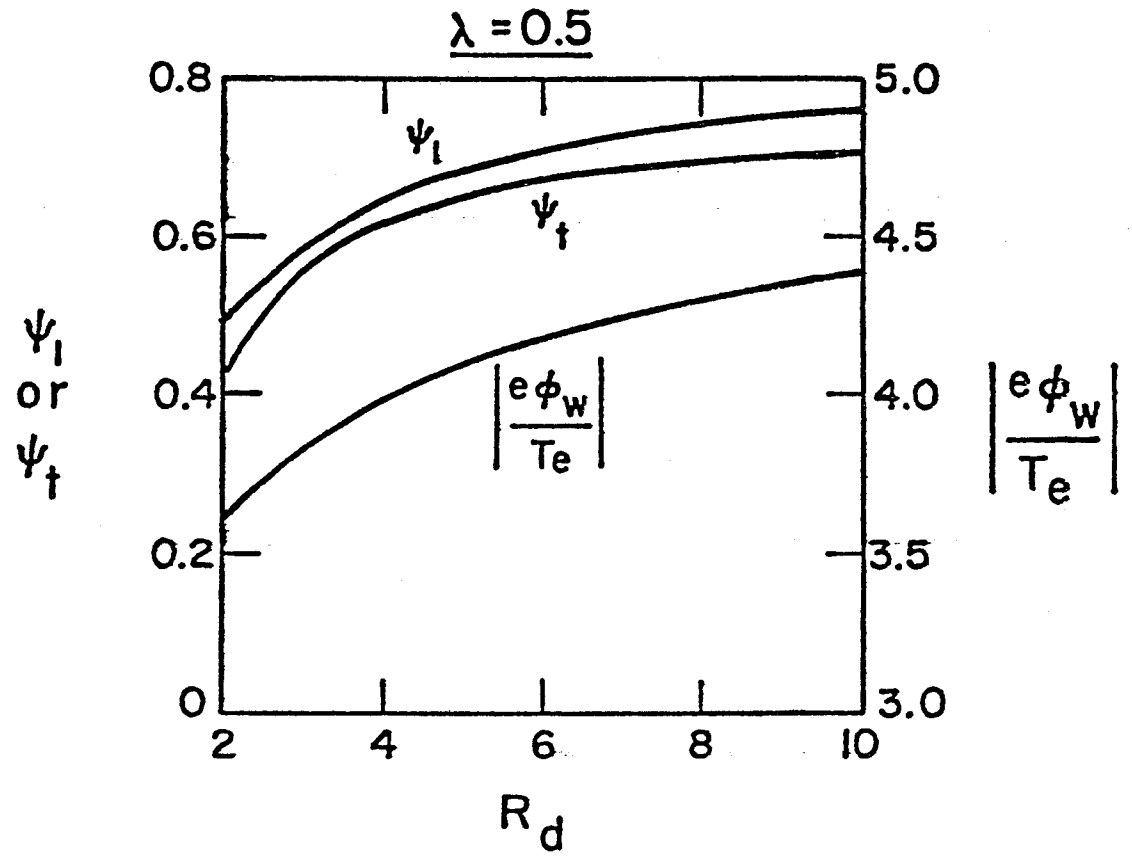

Fig. 4. The effect of the downstream mirror ratio, R_d, on ψ_l, ψ_t, and ϕ_w for $R_u = 2$.